ELSEVIER

Coordination Chemistry Reviews
197 (2000) 169–189

COORDINATION CHEMISTRY REVIEWS

www.elsevier.com/locate/ccr

On the full topology of the Laplacian of the electron density

P.L.A. Popelier *

Department of Chemistry, U.M.I.S.T., 88 Sackville Street, Manchester M60 1QD, UK

Received 26 March 1999; accepted 21 June 1999

Contents

Abstract

In this work we briefly review the use of the function $L(\mathbf{r})$, which is defined as minus the Laplacian of the electron density, $\nabla^2\rho$, in the context of the theory of 'atoms in molecules'. The topology of $L(\mathbf{r})$ can be *almost* faithfully mapped onto the electron pairs of the VSEPR model. The computation of the gradient vector field $L(\mathbf{r})$ opens new avenues for the further quantification of this mapping. Although major questions are still outstanding this contribution explores for the first time the full topology of $L(\mathbf{r})$ for a molecule. In water there are

* Tel.: +44-161-2004511; fax: +44-161-2367677.
E-mail address: pla@umist.ac.uk (P.L.A. Popelier)

PII: S0010-8545(99)00189-7

four regions: the Core Shell Charge Concentration (CSCC), the Core Shell Charge Depletion (CSCD), the Valence Shell Charge Concentration (VSCC) and the Valence Shell Charge Depletion (VSCD). Each region has a set of $L(\boldsymbol{r})$ critical points coagulating in a graph, except the CSCC. In analogy with the topology of the electron density we propose the term *basin interaction line* for the pair of gradient paths linking two basins in $L(\boldsymbol{r})$, and the term *interbasin surface* for the surface separating two basins. We present a systematic study of the water molecule, which possesses 43 critical points in $L(\boldsymbol{r})$. The question is raised how a basin in $L(\boldsymbol{r})$ can be linked with the domain of the VSEPR model.

Keywords: Laplacian of the electron density; Topology of the electron density; Atoms in Molecules; VSEPR

1. Introduction

The theory of 'atoms in molecules' (AIM) [1,2] can be regarded as part of a research program which aims at extracting chemical insight from modern ab initio wave functions. This theory was pioneered by Bader and co-workers in the early 1970s and has since grown into a mature theory, rooted in quantum mechanics [3,4]. On a yearly basis it is used by more than 70 geochemistry laboratories worldwide in areas such as surface science, organometallic chemistry, life science, solid state physics, drug design, physical organic chemistry, crystallography, intermolecular potentials, reaction mechanisms, hydrogen bonding and so forth. In spite of this wide range of application, AIM does not seem to be part of mainstream theoretical chemistry, let alone of current chemical education. However, it is perhaps the only theory which provides a simple, rigorous and elegant definition of two cornerstones of chemistry (for the vast majority of ground state molecules): the atom and the bond [5].

Of course many questions that AIM raises warrant further research, such as the full topology of the Laplacian of the electron density, $\nabla^2\rho$, which is an integral part of AIM. A more ambitious program is to find a convincing and consistent reformulation within the context of AIM of typical chemical concepts such as degree of covalency and ionicity, rotation barriers, the anomeric effect, conjugation and others.

Gillespie was one of the early researchers to take advantage of the novel paradigm of AIM [6] after the first application of the Laplacian to VSEPR was made by Bader, McDougall and Lau in 1984 [17]. Indeed, in the 1980s [7] it was shown that $\nabla^2\rho$ provides a physical basis for the VSEPR model [8,9]. This model is not dependent on the orbital model [10] and is thus compatible with the spirit of AIM. The theory of AIM uses the electron density as its starting point, regardless of how it was obtained. For example, the partitioning of a molecule into atoms, which AIM proposes in terms of the gradient vector field of ρ, can be still be applied to experimental electron densities. In a wider context AIM incorporates quantities which do not trivially depend on ρ, such as the kinetic energy density $K(\boldsymbol{r})$ or the pair density $\rho(\boldsymbol{r}_1, \boldsymbol{r}_2)$. In the absence of the perfect density functional

these quantities can only be obtained from the wave function. The wave function is expressed in terms of basis functions, which constitute a Hilbert space. It is important to realize that AIM does not retrieve chemical insight from Hilbert space; Hilbert space is merely a means to obtain the wave function, from which scalar functions such as ρ and $\nabla^2\rho$ can be obtained. In other words, AIM starts from the topology of real 3D functions (or 6D for the pair density) to recover chemical insight.

A more recent model introduced by Gillespie, called the ligand closed packing model (LCP) [11], also benefits from AIM via the latter's atomic populations. This model is essentially equivalent to the VSEPR model but it explicitly recognizes the importance of intramolecular interactions between adjacent *nonbonded* atoms. Already in the 1960s Bartell realized the importance of nonbonding interactions [12] but his claim — and that of others — was not widely accepted. One of the reasons is that the interligand radii for ligands attached to carbon are too small for most molecules because they were determined for ligands attached to carbon only. Gillespie and Robinson resurrected Bartell's model, subsequently extended and refined it, encouraged by AIM analyses of the electron distribution. Indeed, according to the AIM charges many molecules (such as BF_3) which are commonly thought of as being covalent are actually predominately ionic [13]. This crucial observation eventually led to regarding complexes as closed packed structures with anion-like ligands around a cation-like central atom. Moreover, the Bartell ligand radii were replaced by specific radii, each depending on the central atom (Be, B, C, Si, P and S) the ligands (N, O, F and Cl) that they are bonded to [11,14]. The LCP model provides a more economic explanation (in terms of Occam's razor) of the geometry of molecules such as BF_3, making Pauling's back-bonding model completely unnecessary [15]. Furthermore, the controversial nature of the bonding in OCF_3^- and ONF_3 is resolved under the LCP model [16]. In summary, the two successful models VSEPR and LCP, both based on a huge number of experimental observations, find their physical basis in AIM, without ever relying on orbital arguments. This fact justifies further research into AIM's orbital-free quantities, such as $\nabla^2\rho$.

In this paper we briefly review the Laplacian of the electron density and its use. Next, we present the water molecule as a case study to investigate the full topology of $\nabla^2\rho$. It will become clear that the Laplacian of this simple molecule already shows a bewildering complexity, which has hitherto not been described. We will show that the previously introduced *atomic graph* [17–19] is actually part of a more complicated structure.

In the following section we reiterate the most relevant topological objects appearing in the electron density, to prepare the ground for the topological objects in $\nabla^2\rho$. In Section 3 we briefly discuss the issue of the localization of electron pairs. In Section 4 we summarize the key applications of the Laplacian, and in the final section we present the details of the full topology of the case study water. We end with a conclusion and a few thoughts on future work. An attempt has been made to make this paper self-contained.

2. The topology of the electron density

The topology of ρ is fully understood [20] and leads to a partitioning scheme, which defines *atoms* inside a molecule or a molecular aggregate via the *gradient vector field*, $\nabla\rho$. This vector field is a collection of *gradient paths*, which are curves in space that follow the direction of steepest ascent in ρ. Therefore a gradient path has a sense; it always originates and terminates at points where $\nabla\rho$ vanishes. These points are called c*ritical points* (CP). The CPs in ρ are special and useful points in the molecule.

How can these CPs be classified? It is easy to see that a function depending on two variables shows three types of CPs: a maximum, a minimum or a saddle point. In three dimensions there are *two* types of saddle points. Critical points occurring in a 3D function, such as ρ, can best be characterized by the eigenvalues λ_i ($i = 1$, 2, 3) of the Hessian of ρ, evaluated at the CP. The Hessian is a 3×3 matrix, denoted by $\nabla\nabla\rho$ and containing all possible second derivatives of ρ with respect to the cartesian position coordinates x, y and z. The *rank* (r) of a CP refers to the number of non-zero eigenvalues and the *signature* (s) is the sum of the signs of the eigenvalues. For example, one type of saddle point has two strictly negative (i.e. non-zero) eigenvalues and one strictly positive one. Consequently, its rank is three, and its signature is $(-1)+(-1)+1=-1$. We conveniently denote this point as a $(3, -1)$ CP, where the first index refers to the rank and the second to the signature. This particular type of CP is called a *bond critical point* because it indicates the existence of a bond between two nuclei of a molecule in an equilibrium geometry. The bond critical points are linked to the nuclei via the so-called *atomic interaction line*. This line consists of a pair of gradient paths, each of which originates at the bond CP and terminates at a nucleus. The set of all atomic interaction lines occurring in a molecule is called the *molecular graph*. Another topologically important object is the *interatomic surface*, which separates two bonded atoms. Again it is a collection of gradient paths, originating at infinity and terminating at the bond CP. Finally, the set of gradient paths terminating at a nucleus is called an *atomic basin* or simply *atom*. It will become clear in Section 5 that each of these topological objects appearing in ρ has a counterpart in $\nabla^2\rho$.

3. The localization of electron pairs and the Laplacian of the electron density

In 1916 Lewis introduced his concept of the electron pair, an idea that still dominates chemical thinking today. He was so strongly convinced about the existence of coupled pairs of electrons that he was inclined to denounce Coulomb's law for small inter-electronic separations, an extreme position he later abandoned. Many decades later we face the question: Can we deduce the localization of electrons in pairs from the wave function? More precisely, are there regions in real space in which there is a high probability of finding two electrons of opposite spin?

The pair density $\rho(\boldsymbol{r}_1, \boldsymbol{r}_2)$ is the actual function that indicates regions of space in which there is a high probability of finding two electrons of opposite spin. It has

been shown that the pair density does not, in general, define regions of space beyond an atomic core in which pairs of electrons are localized [21]. Consequently the ubiquitous Lewis model cannot be rigorously recovered from physics, because the motions of valence electrons are so strongly inter-correlated that the localized electron pair model ceases to afford a suitable description.

Nevertheless a remarkable mapping between local maxima in $L(\boldsymbol{r})$ and assumed electron pairs was observed many years ago [17]. Which property of $L(\boldsymbol{r})$ suggests that the validity of the Lewis model may be justified anyway? In general, the Laplacian of a function measures to what extent this function is locally concentrated or depleted. Via finite difference formulae, one can easily prove [2] that when $\nabla^2\rho < 0$ at a given point, the electron density is locally concentrated, i.e. ρ is locally higher at the given point than at any of its neighbouring points. Conversely, when $\nabla^2\rho > 0$ at a given point ρ is locally depleted and the value of ρ will be higher at any of the given point's neighbours. It is convenient and more natural to introduce the function $L(\boldsymbol{r}) = -\nabla^2\rho$, because then a concentration of electron density corresponds to a positive L value. The following discussion refers to the function $L(\boldsymbol{r})$ rather than the Laplacian itself. For example, a $(3, -3)$ CP is a maximum in $L(\boldsymbol{r})$; this CP would be called a $(3, +3)$ or minimum in $\nabla^2\rho$. In summary, the fact that $L(\boldsymbol{r})$ gauges the concentration of the electron density suggests that $L(\boldsymbol{r})$ could be used to detect electron pair localization. Indeed, the mapping between the electron pairs of the Lewis model (and later the VSEPR model) has proven to be faithful enough (albeit it not perfect) to generate useful applications and new insights.

Localized pairs of electrons, bonding or non-bonding, are not evident in the topology of ρ. They are evident however in another one-electron density function, called the electron localization function (ELF) [22], constructed from kinetic energy contributions. This function reveals the expected number of (electronic) shells in free atoms with a nuclear charge higher than 40. It has been shown that the topology of $\nabla^2\rho$ is homeomorphic to ELF with few exceptions. This remarkable correspondence between the topologies of ELF and $L(\boldsymbol{r})$ corroborates the latter function's trustworthiness in locating electron pairs. However, the pattern of maxima in $L(\boldsymbol{r})$ is superior in recovering the classical Lewis model. In other words, $L(\boldsymbol{r})$ corresponds better to chemical intuition than ELF [23]. It is not clear whether this is due to the arbitrary transformation carried out in ELF's construction to obtain values bounded between 0 and 1. Alternatively ELF could be closer to the truth as a one-electron property density than $L(\boldsymbol{r})$ in *not* recovering the Lewis model. After all, the Lewis model cannot be convincingly recovered from the two-electron pair density.

Compared to ELF the $L(\boldsymbol{r})$ function is very simple and free from arbitrary manipulations during its construction, such as considering only the leading term of the Taylor expansion of the spherically averaged conditional pair probability [22]. In fact, besides its simplicity $L(\boldsymbol{r})$ has a deeper meaning in terms of energy densities. In view of the local virial theorem, $2G(\boldsymbol{r}) + V(\boldsymbol{r}) + \hbar^2/4mL(\boldsymbol{r}) = 0$, where $G(\boldsymbol{r})$ is a kinetic energy density and $V(\boldsymbol{r})$ is the potential energy density, $L(\boldsymbol{r})$ can be interpreted as the local balance between the kinetic and potential energy of a

molecule. Moreover, since an energy density is in fact a pressure one can interpret $\hbar^2/4mL(\boldsymbol{r})$as a local pressure arising in a quantum system.

4. Applications of the Laplacian of the electron density

In this section we discuss the relevance of $L(\boldsymbol{r})$ to chemistry, as $L(\boldsymbol{r})$ has been observed to be useful in practice. We will briefly review how $L(\boldsymbol{r})$ supports the VSEPR model, how $L(\boldsymbol{r})$ reinterprets Lewis acidity and basicity and why $L(\boldsymbol{r})$ is more general than the electrostatic potential map.

The key idea of the first application is to identify the critical points in $L(\boldsymbol{r})$ with the electron pairs in the VSEPR model. This model assumes that the geometrical arrangement of the ligands about a central atom is that which maximizes the separation between the electron pairs or *domains*. An electron pair domain or simply *domain* is the region of space in the valence shell in which the electron pair is most probably to be found [8]. The VSEPR model operates under three postulates. Firstly the lone pair domains are larger than the bonding pair domains. Secondly the change in size of the bonding pair domains is a function of the electronegativity of the ligands and of the central atom. Thirdly the domains of double and triple bonds are larger compared to those of single bonds.

How does AIM then provide a physical basis for VSEPR? The spherical surface along which the lone pairs and ligands move can be identified with the valence shell charge concentration (VSCC) that AIM defines. The VSCC will be precisely defined below but it is basically a zone in the outer region of an atom where $L(\boldsymbol{r}) > 0$. A crude estimate of the size of the local maxima in $L(\boldsymbol{r})$ has been proposed [24] in terms of a simple area of a spherical cap around the atom. This simple measure confirms the three postulates of the VSEPR model in terms of features of $L(\boldsymbol{r})$, but we are confident that this measure can be made more rigorous via $L(\boldsymbol{r})$'s full topology.

The second application of $L(\boldsymbol{r})$ is connected to the Lewis theory of acids and bases. Lewis extended the Brønsted–Lowry acid–base concept and defined an acid as an electrophile and a base as a nucleophile. The adduct F_3B–NH_3 can then be looked upon as a result of the neutralization of the acid BF_3 with the base NH_3. This neutralization principle is paralleled in the topology of $L(\boldsymbol{r})$: a maximum in $L(\boldsymbol{r})$ in the valence shell an atom in one molecule combines with a minimum in $L(\boldsymbol{r})$ in the valence shell of an atom in another molecule. The latter principle has been called the Laplacian complementarity principle [19]. For example, the minima appearing above and below the plane of the nuclei of a keto group form an angle of 110° with respect to the C=O axis, which is the angle predicted for the approach of a nucleophile to a carbonyl carbon from crystallographic data [25]. Similar predictions have been made for the Michael addition reaction [26] and successfully compared with independent potential energy surface calculations. As a final example the geometries of a large number of hydrogen-bonded complexes have been predicted successfully by aligning the maximum in $L(\boldsymbol{r})$ in one monomer with the minimum in $L(\boldsymbol{r})$ in the other monomer. With only a few exceptions, $L(\boldsymbol{r})$ is able

to correctly predict the geometry of a complex of HF with bases such as N_2, CO, CS, CO_2, SCO, HCN, H_2O, H_2S, HF, O_3, H_2CO and many others [27]. However, some more recent work has shown that the quality of the predictive power of $L(\boldsymbol{r})$ diminishes for elements beyond the second row [28–30].

The third application concerns the ability of $L(\boldsymbol{r})$ to predict the preferred sites of protonation of a molecule, which may be of great help in peptide mass spectrometry. This problem can actually be viewed as a special case of the previous point but it is mentioned separately to contrast it with the classical use of the electrostatic potential map [31]. Indeed, the electrostatic potential is actually a potential energy surface of two interacting partners: a molecule and a bare proton. It was shown before that the preferred orientation (*cis* or *trans*) of the proton with respect to the substituent in a dozen carbonyl compounds (XCHO) is generally indicated by the relative magnitude of maxima in the VSCC that are present at the positions of the lone pairs of the oxygen atom [32]. It must be emphasized that whereas the electrostatic potential maps are inherently limited to electrophilic attack, the topology of $L(\boldsymbol{r})$ can be used for both nucleophilic and electrophilic attack.

In summary, the Laplacian is a simple but information-rich function, which acts as a bridge between the wave function and chemical interpretation. The success of its applications warrants a detailed study of its full topology, as explained in the next section.

5. The full topology of $L(\boldsymbol{r})$ for the water molecule

The electron density of a single water molecule possesses five CPs: three maxima, each one almost coincident with a nucleus, and two bond CPs, each one somewhere in between the oxygen and a hydrogen nucleus. The function $L(\boldsymbol{r})$ on the other hand shows a much more complex topology for the same molecule; there are at least 43 CPs. A good starting point to disentangle this plethora of CPs is to look at $L(\boldsymbol{r})$s topology for a free oxygen atom and a free hydrogen atom.

All calculations were performed with the ab initio program Gaussian 94 [33] using the density functional B3LYP [34] and the 6-311 + G(2d, p) [35] basis set. The water molecule was also optimized at this level. The topological analysis was performed using the program MORPHY00 [36] and the 3D pictures were generated using RasMol [37].

5.1. The topology of L(r) for free atoms

Fig. 1 shows the truncated profile of the function $L(r)$ where $\boldsymbol{r}$ is the radial distance from the nucleus for a free spherical oxygen atom in its triplet state. There are four zones in this profile, alternately corresponding to a spherical shell of charge concentration (CC) ($L(\boldsymbol{r}) > 0$) or charge depletion (CD) ($L(\boldsymbol{r}) < 0$). The pair of inner shells constitutes the K-shell or core shell. The pair of outer shells constitutes the L-shell, which is the valence shell. As a result we call the innermost shell the core shell charge concentration (CSCC), the second zone the core shell charge

depletion (CSCD), the third zone the valence shell charge concentration (VSCC) and the fourth zone the valence shell charge depletion (VSCD). This nomenclature is a logical extension of the name VSCC, which the current literature gives to the third zone. The pattern of shells appearing in singlet oxygen is very different.

Table 1 shows seven important radii describing the profile of $L(\boldsymbol{r})$. There are three radii (r_{12}, r_{23}, r_{34}) for which $L(\boldsymbol{r})$ vanishes. They mark the boundaries between the successive shells of charge concentration and depletion. The four remaining radii each describe the position of the extremum in $L(\boldsymbol{r})$ occurring in each shell. For example, the maximum L-value in the VSCC shell is 1.56 au and occurs a distance of 0.71 au from the nucleus. The VSCD on the other hand shows one minimum

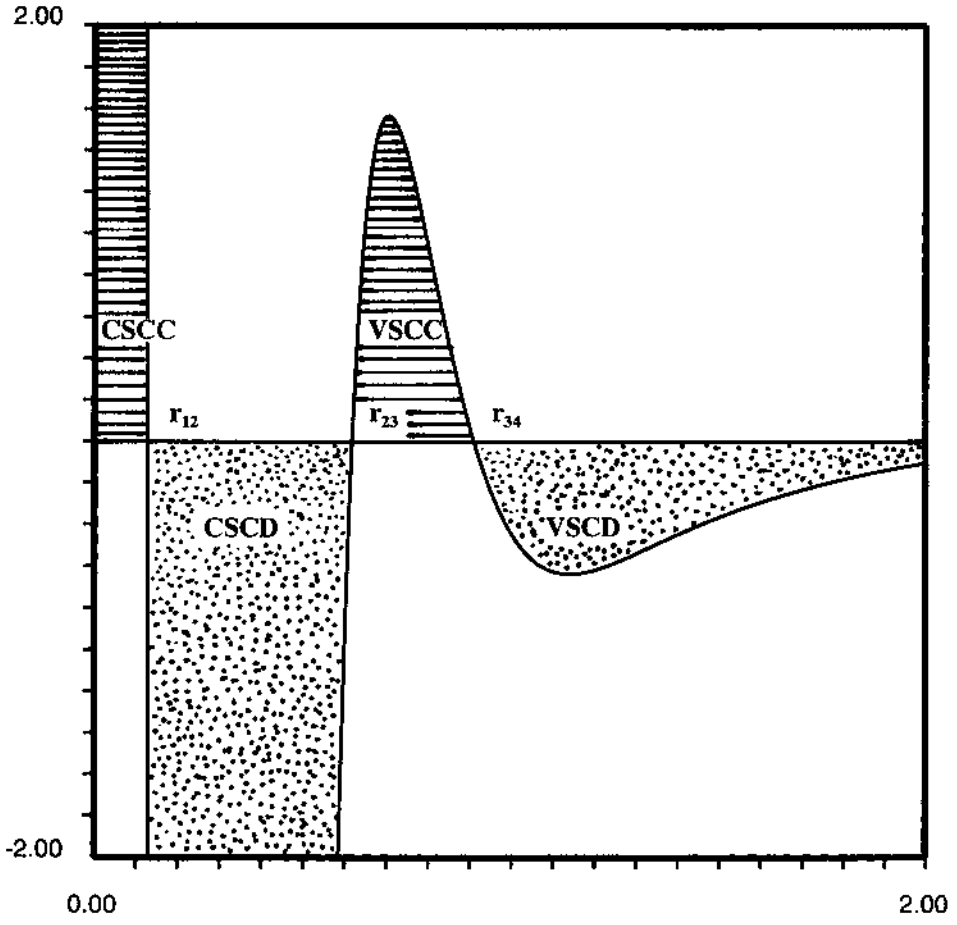

Fig. 1. A truncated representation of $L(\boldsymbol{r})$ (au) versus the radial distance (au) from the nucleus for a free oxygen atom in its triplet state, showing four distinct regions. The two hatched regions are spherical shells of (electronic) charge concentration (CSCC and VSCC), and the two dotted regions are spherical shells of charge depletion (CSCD and VSCD). The marked radii (r_{12}, r_{23}, r_{34}) are the boundaries between the four regions. At these radii $L(\boldsymbol{r})$ vanishes.

Table 1
Values for relevant radii in the $L(\mathbf{r})$ profile of a free oxygen atom in the triplet state

Radius	Value[a]
r_{CSCC}	0
r_{12}[c]	0.13
r_{CSCD}[b]	0.18
r_{23}	0.62
r_{VSCC}	0.71
r_{34}	0.91
r_{VSCD}	1.13

[a] In atomic units.
[b] This is the radius at which the shell's extremum value of $L(\mathbf{r})$ occurs. For CSCC and VSCC this is the maximum value, for CSCD and VSCD this is the minimum value.
[c] This radius is the boundary between zone one and two, i.e. $L(\mathbf{r}_{12}) = 0$. The same convention is applied for the radii r_{23} and r_{34}.

($L = -0.64$ au), rather than a maximum, at a distance of 1.13 au. The numerical information contained in these radii is very important to classify the multitude of CPs occurring in $L(\mathbf{r})$ of water. Indeed, it will become clear that the position of extrema and nodes (i.e. $L(\mathbf{r}) = 0$) is preserved to a large extent in going from the free oxygen atom to oxygen in water.

How can we systematically describe the topology of $L(\mathbf{r})$ for a (spherical) free atom? The outermost part of the topology is a spherical surface of *maximum* charge *depletion* containing an infinite number of $(1, +1)$ CPs, or minima. The radius of this sphere is $r_{VSCD} = 1.13$ au (Table 1). The rank of these CPs is reduced to one because the two eigenvalues corresponding to the plane tangent to the sphere are zero. Indeed, $L(\mathbf{r})$ does not change for a displacement on this tangent plane. Consequently, an extremum or CP in $L(\mathbf{r})$ can be simply described as a one-dimensional minimum or maximum in the radial direction. There is a sphere of maximum charge concentration within this outer sphere. It contains an infinite number of $(1, -1)$ CPs and marks the maximum value of $L(\mathbf{r})$ inside the VSCC. The radius of this sphere is $r_{VSCC} = 0.71$ au (Table 1). The next sphere of $(1, +1)$ CPs is much deeper embedded in the atom's electronic structure. Its radius, denoted by r_{CSCD} amounts to only 0.18 au (Table 1), while the next sphere is shrunk to a zero radius ($r_{CSCC} = 0$). Note that CC shells can only contain maxima and CD shells only minima.

The topology of the hydrogen atom is much simpler as shown in Fig. 2. Since hydrogen has no core we only recover a VSCC and a VSCD zone, which are separated by a nodal sphere (i.e. the set of points where $L(\mathbf{r}) = 0$) with a radius of 1.02 au. It is straightforward to prove that for exact electron densities of one-electron atoms in their ground state this nodal sphere should occur at $r = 1/Z$ where Z is the nuclear charge. So, the calculation with the current basis set introduces an error of 0.02 au since we should have found $r = 1$ au. The $1/Z$ rule is very nearly true for many-electron atoms as well, which is why we expect the radius bounding the CSCC in oxygen to be $1/8 = 0.125$ au instead of the observed value of 0.13 au

(Table 1). In contradistinction to the oxygen, the radii corresponding to the node and the VSCD minimum are both contracted by almost half in going from the free hydrogen atom to hydrogen in water. In conclusion, the oxygen is much less distorted in the formation of a water molecule than a hydrogen.

The question is now, how the atomic topologies survive when atoms combine to form a molecule. Two atoms forming a diatomic molecule reduce the spherical symmetry of their topologies to cylindrical symmetry. As a result the two spherical surfaces of rank-one CPs become a torus of rank-two CPs. A rank-two CP has only one zero eigenvalue which corresponds to the direction tangent to the torus. Formally, we can write $L(\mathbf{r})$ as $L(\rho, \varphi, z)$ where ρ, φ and z are the usual cylindrical coordinates. Because of the cylindrical symmetry $L(\rho, \varphi, z) = L(\rho, z)$, which means

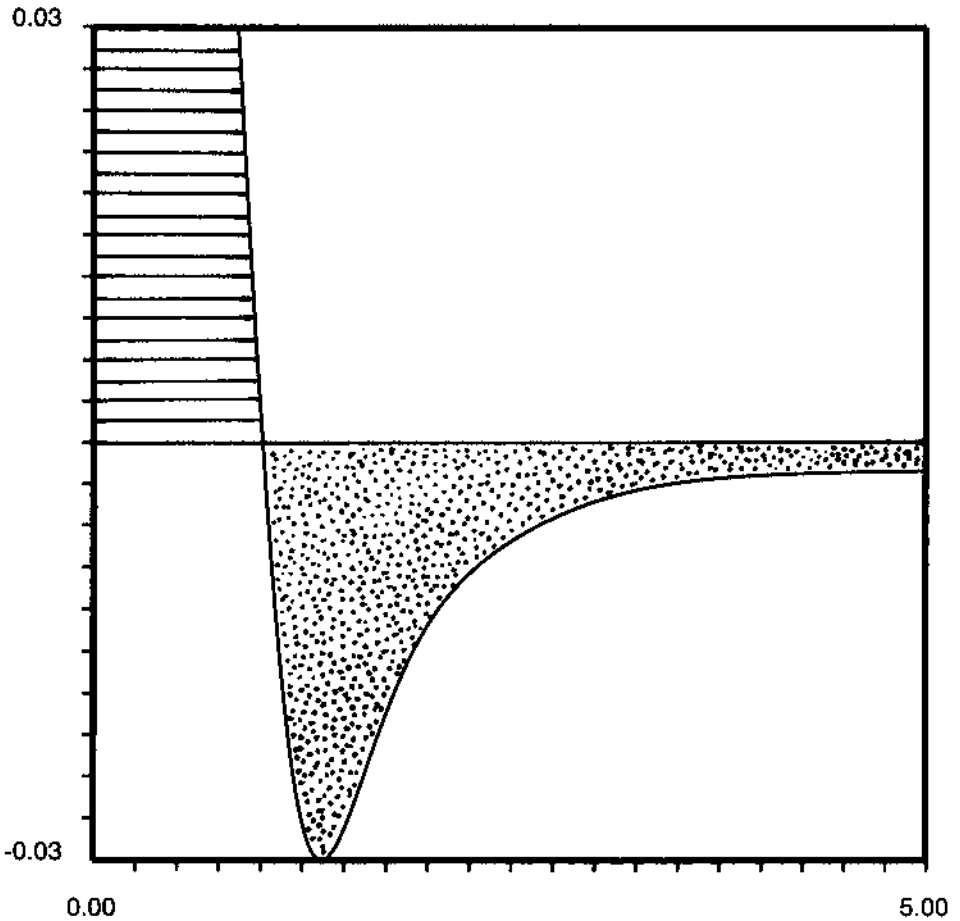

Fig. 2. A truncated representation of $L(\mathbf{r})$ (au) versus the radial distance (au) from the nucleus for a free hydrogen atom, showing two distinct regions. The hatched region is a spherical shell of (electronic) charge concentration (VSCC), and the dotted region is a spherical shells of charge depletion (VSCD).

that L does not depend on φ. In other words, the curvature of L in the direction of φ vanishes and thus the corresponding eigenvalue is zero. Equally, for a free atom, we can write $L(\mathbf{r},\ \theta,\ \varphi) = L(\mathbf{r})$, and the eigenvalues corresponding to a displacement along the two angular coordinates θ and φ are zero. In a less symmetrical molecule such as water, which does not have any angular symmetry, the CPs are of rank three, i.e. there are no directions in which L has a zero curvature.

5.2. Computation of the critical points and the gradient vector field of L

Here we briefly comment on technical issues that arose in this work. The gradient of $L(\mathbf{r})$ is computed from the tensor containing all third derivatives of ρ with respect to the cartesian coordinates x, y, and z, as shown in Eq. (1).

$$\begin{aligned}\nabla L &= \nabla(-\nabla^2\rho) \\ &= -\left[\frac{\partial^3\rho}{\partial x^3}+\frac{\partial^3\rho}{\partial x\partial y^2}+\frac{\partial^3\rho}{\partial x\partial z^2}\right]\boldsymbol{u}_x-\left[\frac{\partial^3\rho}{\partial y\partial x^2}+\frac{\partial^3\rho}{\partial y^3}+\frac{\partial^3\rho}{\partial y\partial z^2}\right]\boldsymbol{u}_y \\ &\quad -\left[\frac{\partial^3\rho}{\partial z\partial x^2}+\frac{\partial^3\rho}{\partial z\partial y^2}+\frac{\partial^3\rho}{\partial z^3}\right]\boldsymbol{u}_z \end{aligned} \tag{1}$$

where $\boldsymbol{u}_x$, $\boldsymbol{u}_y$ and $\boldsymbol{u}_z$ are unit vectors. In order to find the rank and signature of a CP in $L(\mathbf{r})$ one needs to compute the eigenvalues of the Hessian of $L(\mathbf{r})$. In turn this requires the tensor containing the fourth derivatives of ρ with respect to x, y, and z.

Critical points can be located using the Newton–Raphson method but a more robust method called the eigenvector following method [38] is recommended because the topology of $L(\mathbf{r})$ is more challenging. This method is able to find a CP of a given signature starting from a region in space possessing a different signature. The eigenvector following method is part of the program MORPHY98 [39]. In spite of this more robust algorithm, it is very difficult to find critical points in the atomic core region. It is very important to start a CP search within a given interval with *many* intermediate starting radii. In other words, the success of the search is still critically dependent on a good guess of the radius.

The gradient paths in $L(\mathbf{r})$ are computed numerically using the fifth-order Runge–Kutta–Cash–Karp method with adaptive step size control and tolerance $\varepsilon = 10^{-5}$ [40]. Topological objects, such as an attractor's basin or a separatrix (e.g. interatomic surface) is typically generated from a circle or ball of initial points. In some cases a uniform distribution of initial points leads to a bundle of gradient paths avoiding certain parts of space. This problem is well-known in the analytical construction of interatomic surfaces and urged the development of a more sophisticated algorithm for atomic integration [41]. The reason why gradient paths may bundle up in strands (i.e. avoid parts of space) can be understood from the analytical expression for a gradient path's trajectory in the vicinity of a CP [42]. Essentially, the local expression [1] for a gradient path near a CP is:

$$\boldsymbol{r}(s) = \sum_{i=1}^{3} c_i \boldsymbol{u}_i e^{\lambda_i s} \tag{2}$$

where $\boldsymbol{r}(s)$ is the position vector of a point on the gradient path, s is the independent path parameter, c_i are arbitrary constants, u_i are the eigenvectors and λ_i are the eigenvalues of the Hessian of $L(\boldsymbol{r})$. Suppose we have at least two negative eigenvalues, which differ substantially in magnitude (e.g. between a factor of 10 and 100). If we trace the gradient path backwards then s varies from zero (at the initial point) to $-\infty$. It is clear that $\exp(\lambda_1 s) \gg \exp(\lambda_2 s)$ if $\lambda_1 \ll \lambda_2 < 0$. Therefore, the gradient path will evolve much more in the direction of the first eigenvector rather than the second eigenvector. Put differently, the path will always move in the direction of the hard (i.e. large) rather than the soft curvature. Where this phenomenon poses a non-trivial problem for interatomic surfaces, it can be remedied in the construction of an attractor's basin by using an adapted grid of well-sampled initial points.

5.3. The valence shell charge concentration graph

Fig. 3 shows the geometric positions of all the CPs in the VSCC of water. The VSCC of the oxygen atom and of the hydrogen atom have merged into one contiguous region encompassing all three nuclei. This contiguous VSCC contains 16 CPs in total, i.e. six (3, −3) CPs, seven (3, −1) CPs and three (3, +1) CPs. The VSCC can never contain a (3, +3) CP because this would imply that the CP is a minimum even in the radial direction. Since the free atomic shell structure is essentially preserved inside a molecule this is impossible.

The set of (3, −3) CPs falls apart in three subsets: the two nonbonding maxima of oxygen, two bonding maxima between oxygen and hydrogen, and two nuclear maxima, each almost coincident with the hydrogen nucleus (separation of only 0.007 au), and therefore not explicitly shown in Fig. 3. In line with the VSEPR model each nonbonding maximum of oxygen can be identified with a lone pair, and each bonding maximum with the Lewis electron pair in an O–H bond. The existence of an extra maximum very near the hydrogen nucleus is usually ignored and does not find an interpretation within the context of the VSEPR model. Although these extra maxima cannot be regarded as extra electron pairs there are

Fig. 3. The VSCC graph for water. The oxygen nucleus is marked in red and the hydrogen nucleus in white. The (3, −3) CPs (maxima) in $L(\boldsymbol{r})$ are marked in green, the (3, −1) CPs in purple and the (3, +1) CPs in yellow. The (3, −3) CP near each hydrogen nucleus is not shown because it almost coincides with the nucleus. The domain interaction lines (white) link two (3, −3) CPs via a (3, −1) CP.
Fig. 5. The VSCD graph for water. The oxygen nucleus is marked in red and the hydrogen nucleus in white. The (3, +3) CPs (minima) in $L(\boldsymbol{r})$ are marked in brown, the (3, −1) CPs in purple and the (3, +1) CPs in yellow. The (3, +1) CPs link the (3, +3) CPs via a pair of gradient paths (white), each of which is repelled by a (3, +3) CP.

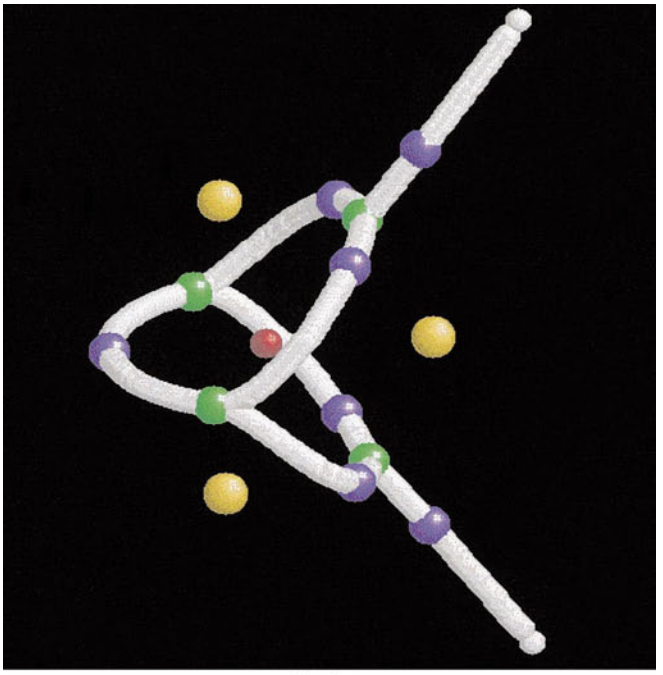

Fig. 3

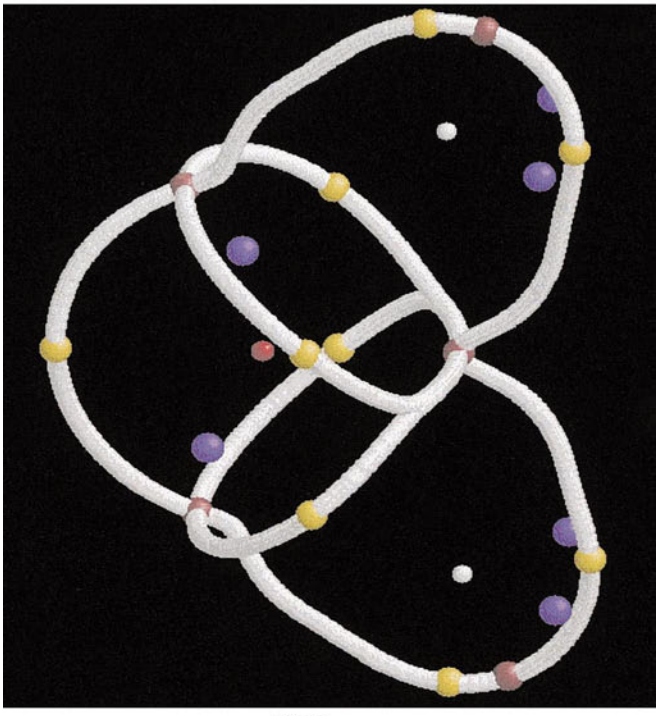

Fig. 5

Figs. 3 and 5.

not much of a practical nuisance. They merely warn us that the correspondence between the topology of $L(\mathbf{r})$ and the VSEPR model is only approximately faithful and may break down. This actually happens in a more dramatic way in inorganic oxides such as $(H_3Si)_2O$ [43], fluorides such as PF_3 and transition metal complexes [44].

The (3, −1) CPs have a function which is analogous to a bond critical point, i.e. to link maxima, which typically (but not necessarily) almost coincide with nuclear positions. Entirely parallel to the construction of an atomic interaction line in ρ, it is possible to trace gradient paths in $L(\mathbf{r})$ starting from the (3, −1) CP. We propose to call this pair of gradient paths in $L(\mathbf{r})$ which link two maxima in $L(\mathbf{r})$ a *basin interaction line*. Of course there are as many basin interaction lines as there are (3, −1) CPs.

The (3, +1) CPs act as minima in the VSCC and are formally equivalent to ring critical points in ρ. Although not shown in Fig. 3 they are linked to (3, −3) and (3, −1) CPs via gradient paths. The collection of such gradient paths forms a topological object which is analogous to the ring surface in the electron density.

The computation of gradients paths enables one to know how the CPs are linked in a network that is usually called the atomic graph. Since the VSCD and the CSCD also contain a graph, we propose the name *valence shell charge concentration* (*VSCC*) *graph* for the set of connected CPs shown in Fig. 3. Fig. 4 shows a compact and convenient representation of the VSCC graph in the plane. The vertices correspond to the (3, −3) CPs, the edges to basin interaction lines (and their (3, −1) CPs), and the faces to the (3, +1) CPs (and the concomitant ring surfaces in $L(\mathbf{r})$). If we assign the symbol V to the number of vertices, E to the number of edges and F to the number of faces of a charge concentration graph then we find that:

$$V - E + F = 2 \tag{3}$$

This formula is a special case of the Poincaré–Hopf relationship [45]. According to Euler, a graph which obeys Eq. (3) is a planar graph [46]. This is a graph that can be drawn in a plane such that none of its edges cross each other. The VSCC graph of a trigonal and tetrahedral carbon also obey Eq. (3) [19]. It should be noted that there is no basin interaction line between the two bonding (3, −3) CPs, but each lone pair (non-bonding) maximum is connected to the other non-bonding maximum and both bonding maxima. Table 2 summarizes all the CPs occurring in the VSCC

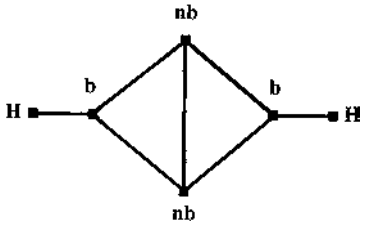

Fig. 4. The planar graph representation of the VSCC graph of water (Fig. 3). This graph has six vertices (squares), seven edges and three faces. A vertex corresponds to a maximum in $L(\mathbf{r})$, an edge to a (3, −1) CP and a face to a (3, +1) CP. The two non-bonding vertices (nb, top and bottom) are linked to each other and to both bonding vertices of oxygen (b, left and right).

Table 2
Quantitative information on all CPs of the VSCC graph of water[a]

Label	type	Comment	Radius	$L(\boldsymbol{r})$	Multiplicity
1, 2	(3, −3)	Non-bonding CP, near O	0.648	5.11	2
3, 4	(3, −3)	Bonding CP, between O and H	0.714	3.01	2
5, 6	(3, −3)	Almost coincident with H	0.007	26.23	2
7, 8, 9, 10	(3, −1)	Links two bonding CPs	0.698	2.79	4
11	(3, −1)	Links two non-bonding CPs	0.657	4.19	1
12, 13	(3, −1)	Links bonding CP with H (3, −3) CP	0.713	0.78	2
14, 15	(3, +1)	In water plane, above and below O	0.702	1.56	2
16	(3, +1)	On C_2 axis, right of O	0.715	1.31	1

[a] Critical points which can be obtained via a symmetry operation of the point group C_{2v} have been omitted. The radius is the distance to the closest nucleus. Comments may refer to Fig. 3.

graph, listing their signature, their radius (i.e. distance from the nearest nucleus) and the value of $L(\boldsymbol{r})$, and their multiplicity in connection with the symmetry operations of water's point group, C_{2v}.

5.4. The valence shell charge depletion graph

This VSCD is also extending over the whole molecule and contains 20 CPs in total, i.e. five (3, +3) CPs, nine (3, +1) CPs and six (3, −1) CPs. The VSCD can never contain a (3, −3) CP because this would imply that the CP is a maximum even in the radial direction. This set of connected CPs can be collectively called the valence shell charge depletion (VSCD) graph. This graph is much more complex than the VSCC graph and encompasses the whole water molecule, as shown in Fig. 5. It is instructive to think of a VSCD graph as a mirror image of a VSCC graph by replacing every positive sign in the eigenvalue spectrum of a CP by a negative sign and vice versa. For example, a (3, −3) CP in the VSCC graph becomes a (3, +3) CP in the VSCD because all three minus signs are replaced by plus signs. Equally, a (3, −1) CP in the VSCC corresponds to a (3, +1) CP in the VSCD and vice versa. As a result, it is now the (3, +1) CP that links the (3, +3) CPs and the (3, −1) CPs represent the faces (or ring surfaces). Another difference is that the gradient paths are repelled (by the (3, +3) CPs) rather than attracted.

Table 3 summarizes all the CPs in the VSCD graph in the same way Table 2 does for the VSCC graph. If we identify the vertices of the VSCD graph with the (3, +3) CPs, the edges with the (3, +1) CPs and the faces with the (3, −1) CPs, then Eq. (3) is also valid for this graph, since $5-9+6=2$.

The VSCC graph and the VSCD have been presented as separate units but of course they are linked by gradient paths as well. A very interesting extension of this work would be to investigate how both graphs change upon a distortion of the nuclear skeleton from the equilibrium geometry. Structural changes in the topology of ρ have been investigated before [47], but is unknown terrain for $L(\boldsymbol{r})$. It is likely that CPs of the VSCC graph and the VSCD graph annihilate each other, a process that may shed light on the absence of bonding maxima in fluorides such as PF_3.

Table 3
Quantitative information on all CPs of the VSCD graph of water[a]

Label	Type	Comment	Radius	$L(\mathbf{r})$	Multiplicity
1, 2	(3, +3)	Near H	0.703	−0.175	2
3, 4	(3, +3)	Near O, above and below, left	1.134	−0.731	2
5	(3, +3)	Near O, on C_2 axis, right	1.137	−0.742	1
6, 7	(3, +1)	Near H, utmost top and bottom	0.712	−0.174	2
8, 9	(3, +1)	Near H, right	0.741	−0.153	2
10	(3, +1)	Near O, utmost left, in water plane	1.179	−0.600	1
11, 12, 13, 14	(3, +1)	Near O, middle	1.180	−0.591	4
15, 16	(3, −1)	Near O, left	1.195	−0.666	2
17, 18, 19, 20	(3, −1)	Near H, right	0.743	−0.152	4

[a] Critical points which can be obtained via a symmetry operation of the point group C_{2v} have been omitted. The radius is the distance to the closest nucleus. Comments refer to Fig. 5.

5.5. The core shell charge depletion graph

The CSCD graph turns out to be rather simple as shown in Fig. 6. This graph is wrapped around the oxygen nucleus rather than the whole molecule and contains six CPs in total, i.e. two (3, +3) CPs, two (3, +1) CPs and two (3, −1) CPs. Again, the number of CPs obeys Eq. (3). Quantitative details of the CPs are listed in Table 4. After many searches we had to conclude that the CSCC has a trivial topology: just one (3, −3) CP in the bisector plane, shifted from the oxygen nucleus towards the protons by only 1.1×10^{-6} au. This brings the total count of CPs to 43. It is not possible to guarantee that all CPs have been located, but one can test if the number and types of CPs found are compatible. The Poincaré–Hopf relationship for $L(\mathbf{r})$, obtained after modifying the one for ρ, becomes

$$n(3, -3) - n(3, -1) + n(3, +1) - n(3, +3) = -1 \quad (4)$$

where $n(3, m)$ is the number of $(3, m)$ CPs ($m = -3, -1, +1, +3$). Indeed, we obtain that $(1 + 6) - (2 + 7 + 6) + (2 + 3 + 9) - (2 + 5) = 7 - 15 + 14 - 7 = -1$.

Fig. 6. The CSCD graph around the oxygen nucleus in water. The oxygen nucleus is marked in red and the hydrogen nucleus in white. The (3, +3) CPs (minima) in $L(\mathbf{r})$ are marked in brown, the (3, −1) CPs in purple and the (3, +1) CPs is yellow. The (3, +1) CPs link the (3, +3) CPs via a pair gradient paths (white), each of which is repelled by the (3, +3) CPs.

Fig. 8. A representation of the basin (blue) belonging to a non-bonding (3, −3) CP in water. This CP acts as an attractor for a multitude of gradient paths in $L(\mathbf{r})$ (blue). The white bowl-shaped object below is the interbasin surface of the (3, −1) CP (purple). This surface separates the basin of one of oxygen's bonding (3, −3) CP (green) and the basin of hydrogen's (3, −3) CP (not shown because almost coincident with the hydrogen nucleus). The VSCC graph of Fig. 3 has been added for reference. Note that the (3, +1) CPs (yellow) are in the plane of water.

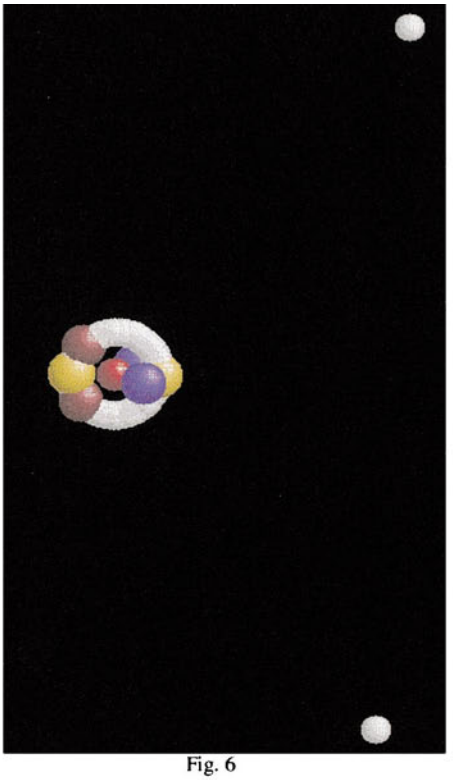

Fig. 6

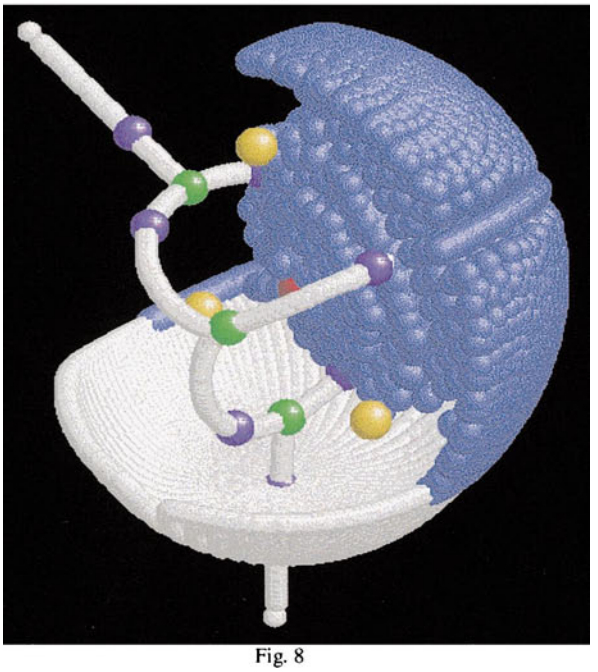

Fig. 8

Figs. 6 and 8.

Table 4
Quantitative information on all CPs of the CSCD graph of water[a]

Labels	Type	Comment	Radius	$L(\boldsymbol{r})$	Multiplicity
1, 2	(3, +3)	In water plane	0.173	−1416	2
3	(3, +1)	On C_2 axis, left of O	0.173	−1414	1
4	(3, +1)	On C_2 axis, right of O	0.175	−1347	1
5, 6	(3, −1)	Front and back	0.174	−1342	2

[a] Critical points which can be obtained via a symmetry operation of the point group C_{2v} have been omitted. Comments refer to Fig. 6.

5.6. The gradient vector field of $L(\boldsymbol{r})$ and domains

In Fig. 7 we show the gradient vector field of $L(\boldsymbol{r})$ in the plane of the water molecule superimposed on the contour map of $L(\boldsymbol{r})$. The CSCC appears as an almost perfectly spherical region centered at the oxygen nucleus, encapsulated by the slightly distorted CSCD. The VSCC is one contiguous zone wrapped around all three nuclei, and also encapsulated, now by the VSCD, which extends to infinity.

Clearly the gradient paths are everywhere perpendicular to the contour lines (except for CPs). The 20 CPs of the valence shell (both VSCC and VSCD) that lie in the plotting plane are also marked. It is clear that the CPs appear with nearly constant radii around there nearest nucleus. The gradient vector field shows the basin in $L(\boldsymbol{r})$ dominated by the (3, −3) CP practically coincident (and therefore not shown) with the hydrogen nucleus. There is also a basin dominated by the bonding (3, −3) CP between O and H. For the sake of clarity we have not shown too many gradient paths, otherwise the attractor pattern would appear more clearly in the gradient vector field. Equally, the nonbonding (3, −3) CP (not shown in Fig. 7) is an attractor for another basin in $L(\boldsymbol{r})$.

An important question is the chemical meaning of the basin in $L(\boldsymbol{r})$. With an eye on the VSEPR model it would be tempting to call such a basin a domain but this proposal yields two problems. Firstly, a basin contains regions where $L(\boldsymbol{r}) > 0$ as well regions where $L(\boldsymbol{r}) < 0$. This means that an electron domain would contain regions of charge depletion. The second problem is that the (large) basin centered on each hydrogen nucleus cannot be explained in terms of VSEPR domains. Also, at the current stage of research it is not clear what the chemical meaning is of the region of space spanned by an infinite number of gradient paths repelled by a (3, +3) CP. In view of the mirror image relationship between CC and CD zones, these regions of space could be called *anti-domains*. Topologically these are exactly the opposite of the domains of the VSEPR model, but to our knowledge anti-domains have no equivalent in the VSEPR model. In summary, the occasional mismatch between $L(\boldsymbol{r})$s topology and VSEPR is a challenge to both VSEPR and AIM. Does VSEPR explains the right (experimental) data for the wrong reasons, or should AIM provide another function, whose topology supports VSEPR better? Perhaps one could focus on that part of the basins where $L(\boldsymbol{r}) > 0$, in order to define, from AIM, a precise spatial region to be identified with a domain.

Finally, in Fig. 8 we produce a 3D view of the basin in $L(\boldsymbol{r})$ (blue) corresponding to the non-bonding (lone pair) $(3, -3)$ CP. In future work the volume of such a region will be computed as well as its charge by integrating the electron density over this volume.

In Fig. 8 we also show the topological analogue of the interatomic surface. In $L(\boldsymbol{r})$ it is the boundary between two basins and can therefore be simply called an *interbasin surface*. The white bowl-shaped object at the bottom of Fig. 8 is the interbasin surface of the $(3, -1)$ CP between the basin of a hydrogen and a bonding basin of oxygen.

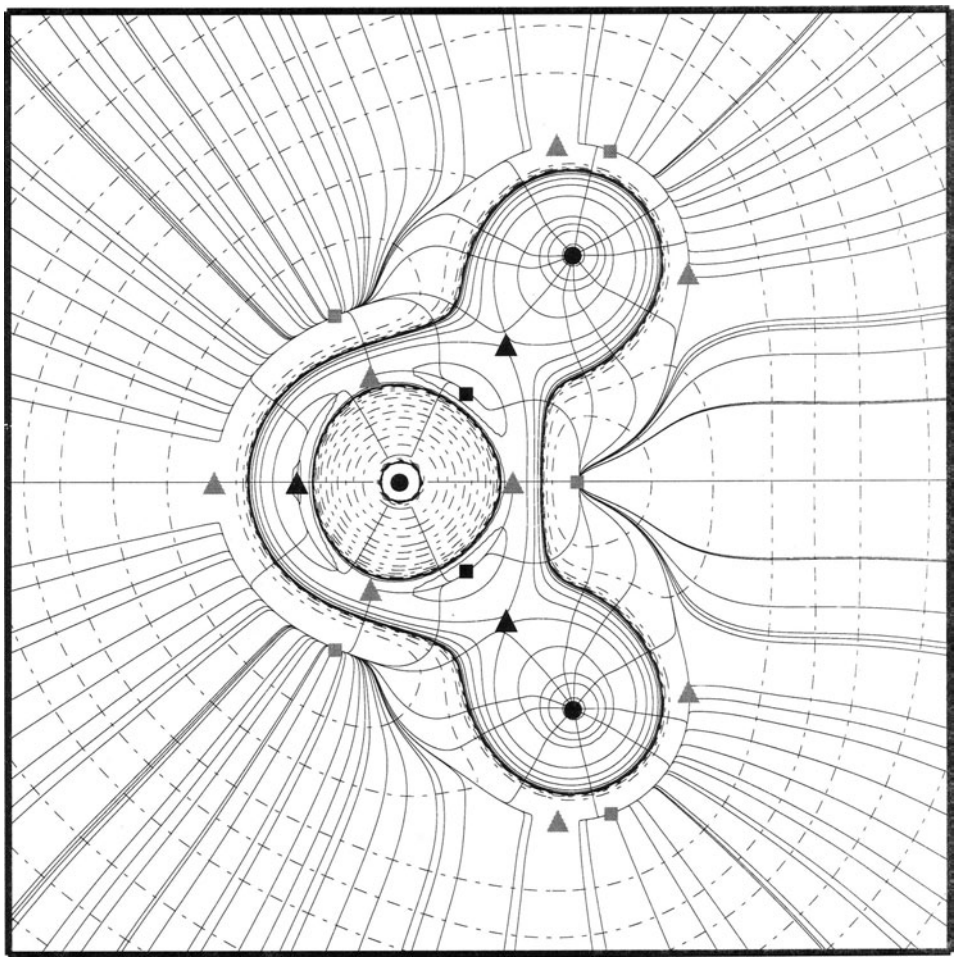

Fig. 7. A superposition of the gradient vector field of $L(\boldsymbol{r})$ and its contour map in the plane of the water molecule. The dashed contour lines correspond to negative $L(\boldsymbol{r})$ values (electronic charge depletion). The solid squares mark $(3, -3)$ CPs, the solid triangles $(3, -1)$ CPs, gray triangles $(3, +1)$ CPs and gray squares $(3, +3)$ CPs. Only the CPs belonging to the valence shell have been marked.

The interbasin surface can be constructed by tracing gradient paths backward (i.e. steepest descent) from a small circle of initial points around the (3, −1) CP. In general, good representations of other interbasin surfaces are hard to generate because of the technical difficulties that largely differing Hessian eigenvalues generate (see Section 5.2).

6. Conclusion

An exploratory investigation into the full topology of $L(\boldsymbol{r})$ has been performed for water. Even for such a simple molecule the complexity of the topology of $L(\boldsymbol{r})$ is bewildering compared to that of ρ. Nevertheless this set of critical points can be understood from the topology of the free atoms participating in the molecule under study. The consecutive regions of electronic charge concentrations and charge depletion of both core and valence shell are largely preserved for oxygen, in going from the free to the bonded atom. Each such region (except the CSCC) has a connectivity scheme of critical points, linked by the so-called interbasin lines. This scheme can be compactly represented by a planar graph, which is convenient for classification purposes in a chemical database of quantum atoms. The function $L(\boldsymbol{r})$ has been proven to be of practical use in chemistry, not in the least because of the almost faithful mapping its topology has with the VSEPR model.

Recently, however, the VSEPR model has been reformulated and it still is in a continuous state of refinement and updating. To quote Gillespie (1996) 'In its original formulation, the model was based on the concept that valence shell electron pairs behave as if they repel each other and thus keep as far apart as possible. But in recent years more emphasis has been placed on the space occupied by a valence shell electron pair, called the domain of the electron pair, and on the relative sizes and shapes of these domains' [8]. This shift in emphasis has been one of the incentives to embark on the study of $L(\boldsymbol{r})$'s full topology. Clearly, future research faces the continuing challenge of preserving the much desired link between VSEPR and the physics governing a molecule. A recent study on electron localization concluded that one may begin to understand how information regarding the pair density is transmitted to $L(\boldsymbol{r})$ in terms of the behavior of the so-called Lennard–Jones function [48]. We have planned a systematic study of $L(\boldsymbol{r})$'s topology of more involved compounds, such as ClF_3, SF_4, SF_4O, ClF_5 and SF_6 and possibly a transition metal complex in order to understand the correspondence between VSEPR and AIM better.

References

[1] R.F.W. Bader, Atoms in Molecules. A Quantum Theory, Clarendon, Oxford, 1990.
[2] P.L.A. Popelier, Atoms in Molecules. An Introduction, Pearson Education, Harlow, UK, 1999.
[3] R.F.W. Bader, Pure Appl. Chem. 60 (1988) 145.
[4] R.F.W. Bader, Chem. Rev. 91 (1991) 893.
[5] P.L.A. Popelier, Sci. Comput. World 45 (1999) 26.

[6] R.F.W. Bader, P.L.A. Popelier, T. Keith, Angew. Chem. Int. Ed. Engl. 33 (1994) 620.
[7] R.F.W. Bader, R.J. Gillespie, P.J. MacDougall, J. Am. Chem. Soc. 110 (1988) 7329.
[8] R.J. Gillespie, E.A. Robinson, Angew. Chem. Int. Ed. Engl. 35 (1996) 495.
[9] R.J. Gillespie, I. Hargittai, The VSEPR Model of Molecular Geometry, Allyn and Bacon, London, 1991.
[10] R.J. Gillespie, Struct. Chem. 9 (1998) 73.
[11] R.J. Gillespie, E.A. Robinson, Adv. Mol. Struct. Res. 4 (1998) 1.
[12] L.S. Bartell, J. Chem. Phys. 32 (1960) 827.
[13] E.A. Robinson, S.A. Johnson, T.-H. Tang, R.J. Gillespie, Inorg. Chem. 36 (1997) 3022.
[14] R.J. Gillespie, I. Bytheway, E.A. Robinson, Inorg. Chem. 37 (1998) 2811.
[15] R.J. Gillespie, J. Chem. Educ. 75 (1998) 923.
[16] R.J. Gillespie, E.A. Robinson, G.L. Heard, Inorg. Chem. 37 (1998) 6884.
[17] R.F.W. Bader, P.J. MacDougall, C.D.H. Lau, J. Am. Chem. Soc. 106 (1984) 1594.
[18] R.F.W. Bader, C. Chang, J. Phys. Chem. 93 (1989) 2946.
[19] R.F.W. Bader, P.L.A. Popelier, C. Chang, J. Mol. Struct. (Theochem.) 255 (1992) 145.
[20] R.F.W. Bader, Acc. Chem. Res. 18 (1985) 9.
[21] R.F.W. Bader, M.E. Stephens, J. Am. Chem. Soc. 97 (1975) 7391.
[22] A.D. Becke, K.E. Edgecombe, J. Chem. Phys. 92 (1990) 5397.
[23] R.F.W. Bader, S. Johnson, T.-H. Tang, P.L.A. Popelier, J. Phys. Chem. 100 (1996) 15398.
[24] R.F.W. Bader, H. Essen, J. Chem. Phys. 80 (1984) 1943.
[25] H.B. Buergi, J.D. Dunitz, Acc. Chem. Res. 16 (1983) 153.
[26] M.T. Carroll, J.R. Cheeseman, R. Osman, H. Weinstein, J. Phys. Chem. 93 (1989) 5120.
[27] M.T. Carroll, R.F.W. Bader, Mol. Phys. 65 (1988) 695.
[28] S.T. Howard, J.P. Foreman, P.G. Edwards, Can. J. Chem. 75 (1997) 60.
[29] S.T. Howard, J.A. Platts, J. Phys. Chem. 99 (1995) 9027.
[30] J.A. Platts, S.T. Howard, B.R.F. Bracke, J. Am. Chem. Soc. 118 (1996) 2726.
[31] P. Politzer, J.S. Murray, in: B. Lipkowitz (Ed.), Reviews in Computing Chemistry, vol. 2, VCH, NewYork, 1992, p. 273.
[32] T. Slee, R.F.W. Bader, J. Mol. Struct. (Theochem.) 255 (1992) 173.
[33] Gaussian, M.J. Frisch, G.W. Trucks, H.B. Schlegel, P.M.W. Gill, B.G. Johnson, M.A. Robb, J.R. Cheeseman, T. Keith, G.A. Petersson, J.A. Montgomery, K. Raghavachari, M.A. Al-Laham, V.G. Zakrzewski, J.V. Ortiz, J.B. Foresman, J. Cioslowski, B.B. Stefanov, A. Nanayakkara, M. Challacombe, C.Y. Peng, P.Y. Ayala, W. Chen, M.W. Wong, J.L. Andres, E.S. Replogle, R. Gomperts, R.L. Martin, D.J. Fox, J.S. Binkley, D.J. Defrees, J. Baker, J.P. Stewart, M. Head-Gordon, C. Gonzalez, J.A. Pople, Gaussian Inc., Pittsburgh PA, 1995.
[34] A.D. Becke, J. Chem. Phys. 98 (1993) 5648.
[35] J.B. Foresman, Frisch, A., Exploring Chemistry with Electronic Structure Methods, Gaussian, Inc., Pittsburgh, PA, 1996.
[36] P.L.A. Popelier, This program is under development and will not be released until late 2000, 1999.
[37] R. Sayle, RasMol, Glaxo Research, Stevenage, Engl, EU, 1994.
[38] P.L.A. Popelier, Chem. Phys. Lett. 228 (1994) 160.
[39] P.L.A. Popelier, A computer program to perform an automatic AIM analysis. For information on MORPHY98 consult http://www.ch.umist.ac.uk/morphy, 1998.
[40] W.H. Press, S.A. Teukolsky, W.T. Vetterling, B.P. Flannery, Numerical Recipes in FORTRAN, Cambridge University, Cambridge, 1992.
[41] P.L.A. Popelier, Comp. Phys. Comm. 108 (1998) 180.
[42] P.L.A. Popelier, Theor. Chim. Acta 87 (1994) 465.
[43] R.J. Gillespie, S.A. Johnson, Inorg. Chem. 36 (1997) 3031.
[44] G. Heard, R.J. Gillespie, unpublished work.
[45] K. Collard, G.G. Hall, Int. J. Q. Chem. 12 (1977) 623.
[46] N. Trinajstic, Chemical Graph Theory, vol. 1, CRC, Boca Raton, FL.
[47] R.F.W. Bader, T.T. Nguyen-Dang, Y. Tal, Rep. Program Phys. 44 (1981) 893.
[48] R.J. Gillespie, D. Bayles, J. Platts, G.L. Heard, R.F.W. Bader, J. Phys. Chem. A 102 (1998) 3407.